**ORIGINAL ARTICLE**

Biology

# Spawning ground selection and larval feeding habits of Arabesque greenling *Pleurogrammus azonus* around the Matsumae Peninsula, Japan

Tetsuya Takatsu[1] · Tomoaki Toyonaga[1,3] · Shin'ya Hirao[1,4] · Eri Ooka[1,5] · Naoto Kobayashi[2] · Mitsuhiro Nakaya[1]

**Abstract**

We investigated the geographical distribution and feeding habits of Arabesque greenling *Pleurogrammus azonus* larvae along the Tatehama coast of Hokkaido Japan and its eastern waters from November to February. The goal was to gain insights into choice of spawning grounds and early life history. Yolk-sac larvae were predominantly found in the surface water layer near the Tatehama coast during late January to late February, and they were transported to the offshore regions by the Tsushima-Tsugaru Warm Current. During the early developmental stages, the yolk-sac larvae primarily fed on *Oithona similis* copepodites, which are larger than the copepod nauplii consumed by other marine fish species. Our observations of high feeding activity in the surface layer in offshore deep-water areas led us to hypothesize that the Tatehama coast may serve as a spawning ground for adult *P. azonus* due to its proximity to offshore areas, allowing larvae to quickly reach suitable feeding grounds after hatching. The larger egg diameter, longer body length, larger eyes with guanine pigmentation, coiled digestive system, and heavy body pigmentation of *P. azonus* suggest their ability to prey on copepodites and maintain sustained feeding intensity.

**Keywords** Advection · Coastal topography · Copepodite · Initial feeding · *Oithona similis* · Reproductive strategy · Spawning ground

## Introduction

The survival and population dynamics of many fish species are greatly influenced by fluctuations in their early life stages, including the egg, larval, and juvenile periods. This has led to researchers making significant efforts to understand the factors influencing these stages. Since Hjort's critical period and transport hypotheses were proposed in 1914, various recruitment hypotheses have been suggested, including the match-mismatch hypothesis (Cushing and Dickson 1976), predation hypothesis (Hunter 1981; van der Veer and Bergman 1987), growth and growth-predation

✉ Tetsuya Takatsu
   takatsu@fish.hokudai.ac.jp

   Tomoaki Toyonaga
   toyonagasakura@yahoo.co.jp

   Shin'ya Hirao
   hirao-sinya@hro.or.jp

   Eri Ooka
   eri.o.o.k.a.1203@gmail.com

   Naoto Kobayashi
   kobayasi@fish.hokudai.ac.jp

   Mitsuhiro Nakaya
   mnakaya@fish.hokudai.ac.jp

[1] Graduate School of Fisheries Sciences, Faculty of Fisheries Sciences, Hokkaido University, 3-1-1, Minato, Hakodate, Hokkaido 041-8611, Japan

[2] Training Ship "Ushio-Maru", Faculty of Fisheries, Hokkaido University, 3-1-1, Minato, Hakodate, Hokkaido 041-8611, Japan

[3] Home Logistics Co Ltd, 1-2-39, Shinkotoni7joh, Kita-Ku, Sapporo, Hokkaido 001-0907, Japan

[4] Fisheries Research Department, Abashiri Fisheries Research Institute, Hokkaido Research Organization, 1-1-1, Masuura, Abashiri, Hokkaido 099-3119, Japan

[5] Hakodate City Hall, 4-13, Shinonome, Hakodate, Hokkaido 040-8666, Japan

hypotheses (Houde 1987; Anderson 1988; Litvak and Leggett 1992; Pepin et al. 1992; Watanabe et al. 1995; Campana 1996; Takasuka et al. 2003; Joh et al. 2013; Kano et al. 2015), and the bigger-is-better and maternal effects hypotheses (Miller et al. 1988; Chambers and Waiwood 1996; Kjesbu et al. 1996; Solemdal 1997; Higashitani et al. 2007; Kajiwara et al. 2022). Selective migration by vertical distribution layer (Haldorson et al. 1993; Champalbert and Koutsikopoulos 1995), turbulence (Incze et al. 1996; Porter et al. 2005), irradiance (Olla and Davis 1990; Ponton and Fortier 1992), hatch date-selective mortality (Joh et al. 2009), and low food availability associated with vertical stratification (Nanjo et al. 2017) are also factors that affect survival rates in the early life stages.

Arabesque greenling *Pleurogrammus azonus* is a cold-water demersal fish distributed in the Sea of Japan, Yellow Sea, Primorsky Krai, and the Sea of Okhotsk. Around Hokkaido, *P. azonus* populations are divided into three stocks based on differences in spawning ground and spawning season (Irie 1983), with one of these, the southern-Hokkaido-Honshu stock, distributed around the Tsugaru Strait (Hoshino et al. 2009; Fig. 1). *Pleurogrammus azonus* is caught commercially by set nets, bottom gill nets (Natsume 2003), and basket traps. In Matsumae Town, Hokkaido, the catch of this species decreased from 2354 tons in 1998 to 48 tons in 2021 (Hokkaido Research Organization, Marine Net Hokkaido: https://www.hro.or.jp/list/fisheries/marine/h3mfcd0000000ge0.html). Previous studies have provided scientific descriptions of the biology of immature and adult fish of this species (e.g., Kyushin 1977; Natsume 1995; Hoshino et al. 2009; Takashima et al. 2013; 2016). It is known that adult females of *P. azonus* spawn demersal and adhesive eggs that are 2.5–3.0 mm in diameter and that adult males guard eggs until hatching on rocky coastal areas at depths ranging from 6 to 30 m (Kambara 1957). In Tatehama waters off Matsumae Town, *P. azonus* spawns from mid-November to mid-December (Hirano 1947; Kambara 1957; Fig. 1). The egg period of *P. azonus* is relatively longer than that of other cold-water species, being approximately 44–60 days in water at 12–8 °C (Nakaya et al. 2017). There have been several reports on *P. azonus* larvae and juveniles, collection records in offshore areas (Tsujisaki and Kambara 1958; Okiyama 1965; Kyushin 1977), larval distribution in the Soya Strait (Sano 1984) and in the Sea of Japan off Russia (Davydova et al. 2007), and otolith microstructure (Marannu et al. 2017). Snapshot information on the diet of *P. azonus* pelagic larvae and juveniles is available; they were reported to be feeding mainly on copepods like *Oithona similis* and *Pseudocalanus minutus* in the surface layer of offshore sampling stations at 205- to 2525-m seafloor depths in the Sea of Japan off Russia during the daytime in November 2003 (Davydova et al. 2007). However, the spatiotemporal distribution and diet of *P. azonus* larvae in the spawning coastal area have not been clarified in any area. Feeding is almost the only way of obtaining nutritional intake for fish larvae after yolk-sac absorption, and most newly hatched marine fish larvae have poor swimming ability and are vulnerable to high mortality when transported to areas with unfavorable water temperatures and low food availability. Therefore, it is necessary to elucidate the spatial distribution and feeding conditions during the initial feeding stages and the strength of the environmental factors that influence them to understand the early survival process.

To elucidate the early life history and the mechanism of population fluctuations of *P. azonus*, we investigated the characteristics of the spatiotemporal distribution and prey species of larvae of this species in the coastal and downstream areas off Matsumae Peninsula, Hokkaido Island, one of the spawning grounds, to quantify the environmental factors affecting feeding success. We also aimed to determine the effects of spawning ground selection by adults of this species on the survival of drifting larvae.

## Materials and methods

### Field sampling

A part of the Tsushima Warm Current (TsWC) originating from the Kuroshio Current flows into Tsugaru Strait from its western side and then flows into the Pacific Ocean under the name Tsugaru Warm Current (TgWC; Fig. 1). The TgWC always flows from west to east, i.e., from the Sea of Japan to the Pacific Ocean, except during slack water (Odamaki 1985). A part of the northward-flowing TsWC (the TsWC branch) forms a clockwise current in the water east of Okushiri Island. According to information from local fishermen, the spawning grounds of *P. azonus* are located off the coasts of Tatehama and Matsumae, and the direction of the current is always eastward. Therefore, we set up 30 sampling stations in this area and along the Matsumae Peninsula coast to the east. We conducted surveys for *P. azonus* 2009–2011 year-classes during the daytime using the T/S *Ushio-maru* (179 t) of the Faculty of Fisheries of Hokkaido University and the fishing boat *Yamato-maru* (3.9 t) belonging to the Matsumae Sakura Fishing Cooperative Association (Table 1). However, it was often impossible to perform surveys in regions A and B due to frequent unfavorable weather conditions. Also, the survey was limited to the coastal area because the offshore area (about ≥ 10 km from the Matsumae Peninsula) could not be surveyed by small vessels due to stormy weather caused by the northwest monsoon during the autumn and winter. Surveys in region A on 21 January 2009 and in the B, C, and D regions during 28–29 January 2009 were treated as a single survey because of their close timing.
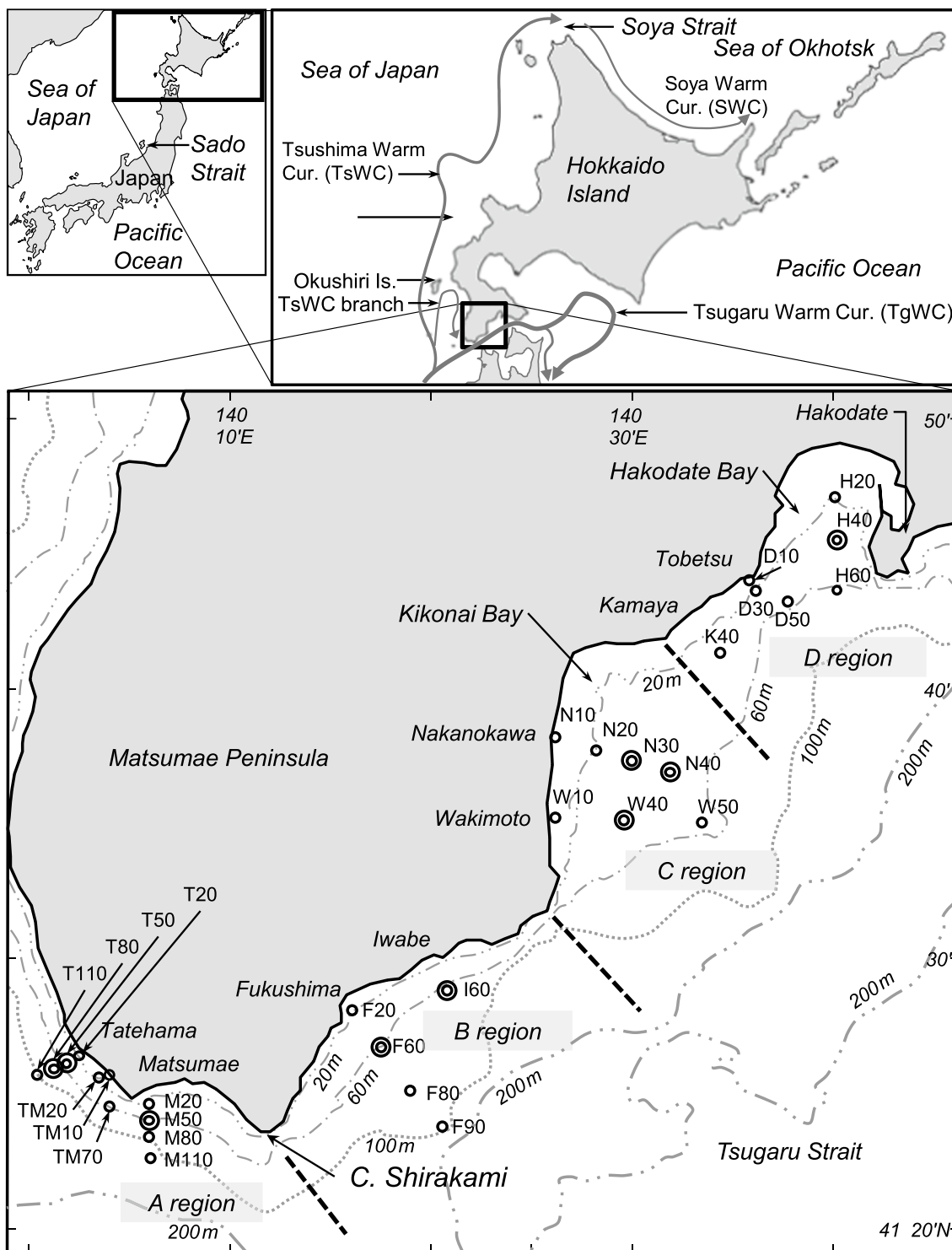
**Fig. 1** Locations of sampling stations around the Matsumae Peninsula. Single circles show the locations of surface tows with a plankton net for larval sampling. Double circles show the locations of surface and 10-m-depth layer tows. Each number at the sampling station indicates the bottom depth in meters. Sampling stations were grouped into four regions: A, B, C, and D, from west to east

*Pleurogrammus azonus* larvae are distributed in the surface layer in Sado Strait (Okiyama 1965; Fig. 1), but no quantitative study has been conducted to compare

the vertical distribution of larvae of this species in other waters. Therefore, in this study, *P. azonus* larvae were collected using a ring net (diameter: 80 cm, mesh aperature:

**Table 1** Sampling station number, samples, and *Pleurogrammus azonus* larvae collected by sampling depth off Matsumae and its eastern downstream area in three spawning years (2009–2011 year-classes)

| Year-class and sampling date | Vessel[a] | Sampling layers (m) | Number of sampling stations | Number of larvae collected | Sea surface temperature (°C)[b] | Sea surface salinity (PSU)[b] | Sea bottom depth (m)[b] | Sea surface density of copepodites excluding *Oncaea* sp. (inds./L)[b] |
|---|---|---|---|---|---|---|---|---|
| *2009 year-class* | | | | | | | | |
| 13 November 2008 | Y | 0, 10 | 8, 1 | 0, 0 | 15.6–15.8–16.0a | 33.84–33.91–33.98b | 17–37–84 | 1.76–4.49–7.21a |
| 27 November 2008 | U | 0, 10 | 6, 1 | 0, 0 | 13.5–13.8–15.3b | 33.89–34.04–34.06a | 32–58–84 | 3.97–5.74–7.50a |
| 24 December 2008 | U | 0, 10 | 8, 3 | 0, 0 | 11.7–12.0–12.3c | 33.69–33.84–33.95b | 6–27–42 | 0.15–1.99–3.97a,b |
| 21 January 2009 | Y | 0 | 7 | 68 | 9.5–10.5–10.8d | 33.81–33.95–33.98a,b | 13–19–23 | 0.29–1.91–2.79b |
| 28–29 January 2009 | U | 0, 10 | 16, 6 | 155, 5 | 7.8–10.2–10.9e | 33.16–34.01–34.10a | 14–4–84 | 0.15–1.69–3.38b |
| 26–27 Feb. 2009 | U | 0, 10 | 18, 7 | 1, 0 | 5.6–6.6–7.9f | 33.76–34.02–34.11a | 15–43–102 | (No data) |
| *2010 year-class* | | | | | | | | |
| 30 November to 1 December 2009 | U | 0, 10 | 24, 4 | 0, 0 | 12.9–14.2–15.8a | 33.00–33.87–33.92b | 13–51–116 | 0.44–3.97–11.91a |
| 21–22 December 2009 | U | 0, 10 | 14, 2 | 5, 0 | 9.4–11.5–12.5b | 33.58–33.89–34.00b | 13–32–64 | 1.62–2.06–5.88a,b |
| 26–27 January 2010 | U | 0, 10 | 12, 2 | 7, 0 | 6.9–8.8–9.7c | 32.99–33.92–34.00b | 13–36–68 | 0.59–1.03–3.97b |
| 18–19 February 2010 | U | 0, 10 | 24, 4 | 242, 2 | 6.7–7.9–8.5d | 33.67–34.03–34.08a | 14–51–114 | 0.00–2.21–6.62a,b |
| *2011 year-class* | | | | | | | | |
| 29 November 2010 | U | 0 | 10 | 0 | 9.9–12.8–13.3a | 32.26–33.61–33.66b | 11–33–67 | 0.00–5.29–11.76a |
| 20–21 December 2010 | U | 0 | 17 | 1 | 11.4–12.4–12.7a | 32.72–33.64–33.77b | 14–41–108 | 1.76–4.63–10.88a |
| 27–28 January 2011 | U | 0 | 24 | 2415 | 6.9–8.7–9.9b | 32.36–33.91–33.98a | 14–44–119 | 0.59–2.13–3.38b |
| 14–15 February 2011 | U | 0 | 24 | 110 | 6.4–7.9–9.3b | 33.64–33.87–33.95a | 16–51–116 | 0.44–2.21–4.26b |

[a]Y, Fishing boat *Yamato-maru*; U, training ship *Ushio-maru*

[b]Values are presented as minimum-median-maximum. Values followed by different lowercase letters indicate significant differences at $p \leq 0.05$ between sampling periods in the same year-class by the Steel–Dwass multiple comparison test

0.33 mm) with a flow meter (Rigo Co Ltd, Tokyo, Japan) by horizontal tows of 10 min at a towing speed of 1.0 m/s in the 0-m-depth surface layer at all sampling stations and in the 10-m-depth layer, for a total of 30 tows at nine sampling stations (Table 1; Fig. 1). In the surface tows, the warp length was adjusted so that no part of the net was exposed from the surface layer. In the 10-m-depth layer, the depth of the ring net was estimated by the warp angle and length, and the warp length was adjusted as needed. Ichthyoplankton specimens, including *P. azonus* larvae, were preserved in 90% ethanol solution to prevent decalcification of hard tissues.

For the estimation of the abundance of prey plankton for *P. azonus* larvae, zooplankton samples were collected with a van-Dorn bottle sampler (6.8 L; Rigo Co Ltd) at the 0-m-depth layer, excluding the sampling on 26–27 February 2009 (Table 1). The sampled water was filtered through a hand net (mesh aperture: 40 µm), and the retained plankton were fixed in a 5% buffered formalin sea water solution. Sea surface water was collected using a bucket at all sampling stations, and water temperature and salinity were measured using a thermometer (Watanabe Keiki Mfg Co Ltd, Tokyo, Japan) and a salinometer (Portasal 8410; Guildline Instruments Ltd, Ontario, Canada), respectively.

## Larval identification and developmental stage

*Pleurogrammus azonus* larvae were identified as described by Nagasawa and Saito (2014), and the different developmental stages were determined and counted using a binocular stereomicroscope (SMZ-10; Nikon Solutions Co Ltd, Tokyo, Japan) in the laboratory. The different development stages were:

– large yolk-sac: ≥ 50% of the length of the yolk-sac from front to back of anus (Fig. 2a);
– middle yolk-sac: between ≥ 20% and < 50% of yolk-sac length (Fig. 2b);
– small yolk-sac: < 20% of yolk-sac length; the yolk-sac is separated from the peritoneum, with most of it hidden within the pectoral fins (Fig. 2c);
– preflexion: larvae with a straight notochord and no yolk-sac;
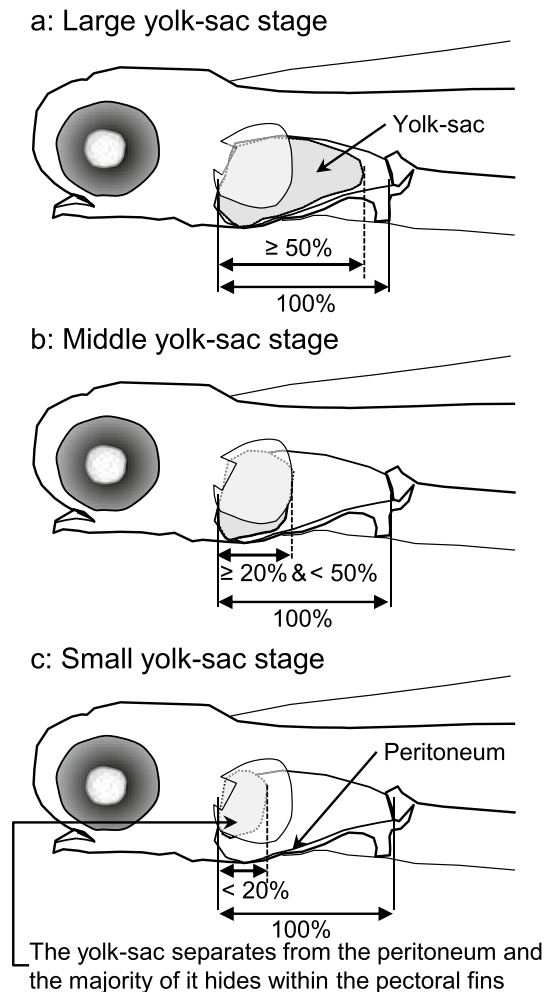
– flexion: larvae in notochord flexion and < 45° to the horizon;
– postflexion: the notochord reaches 45° and the hypural bone achieves ossification.

Because *P. azonus* larvae have open mouths from the time they hatch (Nakaya et al. 2017), larvae with closed mouths were not collected. Notochord length (NL) was measured to the nearest 0.1 mm on all larvae, with the exception of injured larvae, using an electronic caliper (CD-P15S; Mitsutoyo Co., Kawasaki, Japan) or a micrometer on a stereomicroscope. Larval subsamples of *P. azonus* (20 larvae in each subsample) were measured and identified at sampling stations (Stns) T20 and T50 in region A, where considerable numbers of larvae were collected on 17–28 January 2011 (1053 and 1174 individuals [inds.], respectively). Body length shrinkage of *P. azonus* larvae due to preservation in the ethanol solution was not considered in the analysis.

## Dietary analysis

Copepod nauplii and copepodites collected with a van-Dorn bottle were identified to the lowest practical taxa and counted.

*Pleurogrammus azonus* larvae collected on 21 and 28–29 January 2009, 18–19 February 2010, 27–28 January 2011, and 14–15 February 2011, when large numbers of larvae were sampled (hereafter, the four major periods, see Table 1), were subjected to dietary analyses. To exclude larvae that had digested their food during the night, we used larvae collected from 08:07 h (1 h and 15 min after sunrise; sample from 28 January 2009) to 16:59 h (0 h and 14 min before sunset; sample from 28 January 2011) for the dietary analysis. Digestive tracts from the esophagus to the anus were removed, and the contents were identified to the lowest practical taxa and counted. In addition, copepod nauplii in the diet were identified to the genus level in samples collected on 27–28 January 2011. The contents were stained with a methylene blue solution for detecting appendicularians (Takatsu et al. 2007). Three cyclopoid species, *Oithona atlantica*, *O. plumifera*, and *O. longispina*, which are distributed in the study area, were treated together as "*Oithona* spp." because they were unidentifiable under a binocular dissecting microscope.

Comparisons of prey size and estimates of volume were performed for each prey item in the diet using a binocular microscope with an attached micrometer. The dimensions of all prey organisms were exclusive of appendages. The act of being swallowed by a predator is not restricted by the length of the largest prey but usually by the second-largest length (SLL; Pearre 1980). Therefore, SLLs, including body diameters for *Noctiluca* sp., body widths for rotifers, prosome widths for copepod nauplii, prosome depths (for



a: Large yolk-sac stage

Yolk-sac

≥ 50%

100%

b: Middle yolk-sac stage

≥ 20% & < 50%

100%

c: Small yolk-sac stage

Peritoneum

< 20%

100%

The yolk-sac separates from the peritoneum and the majority of it hides within the pectoral fins

**Fig. 2** Three stages of *Pleurogrammus azonus* yolk-sac larvae assessed in this study

*Paracalanus orientalis*, *Pseudocalanus newmani*, and *Pseudocalanus minutus*) or prosome widths (other copepods) for copepodites, shell widths for gastropods, and egg diameters for invertebrate eggs, were used to compare prey sizes (Takatsu et al. 2007). Trunk depth for *Oikopleura* sp. was treated as a SLL because this prey item is usually found in the larval digestive tract as a trunk with house rudiment but without a tail (Takatsu et al. 2007).

Volumes were used for dietary analysis instead of prey weights to avoid under- or overestimation due to differences in digestion speed or weight loss during fixation of the prey organisms (Takatsu et al. 2007). Volumes of prey items were calculated using the geometric formulas of Nishiyama and Hirano (1983) and Takatsu et al. (2007). If an organism was flattened laterally or dorsoventrally, or collapsed in the diet, displacement lengths were calculated using the linear regression formulas between prey lengths from Takatsu et al. (2007) and Hashimoto et al. (2011). Species-specific ratios of prosome volume for copepodites ($m'$ = prosome volume per whole volume; Nishiyama and Hirano 1983) were used (*P. orientalis* as *Paracalanus parvus*: $m'$ = 0.977; *P. newmani*: $m'$ = 0.966, and *Oithona similis*: $m'$ = 0.944; Takatsu et al. 2007). Other $m'$ values were obtained from the mean values of individuals in zooplankton samples collected with a van-Dorn bottle through a 40-μm mesh sieve (*Calanus pacificus*: 0.958 [$n$ = 7]; *Mesocalanus tenuicornis*: 0.961 [$n$ = 5]; *Clausocalanus* sp.: 0.963 [$n$ = 68]; *P. minutus*: 0.971 [$n$ = 7]; *Paraeuchaeta* sp.: 0.943 [$n$ = 6]; *Scolecithricella minor*: 0.986 [$n$ = 5]; *Oithona atlantica* for *Oithona* spp.: 0.916 [$n$ = 11]; *O. oculata*: 0.910 [$n$ = 27]; *Oncaea* sp.: 0.924 [$n$ = 13]). The urosome volumes of *Oithona davisae* and *Eucalanus* sp. were ignored ($m'$ = 1 was adopted for both) because few of these individuals were obtained with the van-Dorn bottle. For unidentifiable calanoid and cyclopoid copepodites, $m'$ values of *P. newmani* and *O. similis* were adopted because *P. newmani* and *O. similis* frequently occurred in the diet (see Results section). If a particle was identifiable but immeasurable due to collapse or digestion (11 out of 5243 prey items), the mean prey lengths of the same prey type in the same digestive tracts were used for volume estimation. In the diet analysis, 76 unidentifiable prey particles were excluded from the volume estimation.

## Data analysis

The density of *P. azonus* larvae (inds./1000 m$^3$) was calculated using the formula:

$$Density_i = N_i \cdot 1000/(A \cdot F_a/F_c) \tag{1}$$

where $N_i$ is the number of larval *P. azonus* individuals collected at station *i*; *A* is the net opening area (m$^2$); $F_a$ is the number of rotations of the flowmeter (rotation); and $F_c$ is the number of rotations per meter in the no-net test (rotations [rot.]/m). For the densities of *P. azonus* larvae in 90 tows during the four major periods (density determined from Eq. 1), the weighted mean bottom-depth of sampling stations (weighted mean depths [WMD]; in meters) and relative bottom-depth to the maximum bottom-depth where *P. azonus* larvae were collected (relative weighted mean depth [RWMD]; in percentage) were calculated by sampling region and period using Eq. 2 and Eq. 3, respectively:

$$WMD = \sum (Density_i \cdot Depth_i)/\sum Density \tag{2}$$

$$RWMD = WMD \cdot 100/(\text{maximum } Depth_i) \tag{3}$$

where $Depth_i$ is the sea-bottom depth where *P. azonus* larvae were collected at station *i* (in meters) by sampling region (A, B, C, and D).

Counts of copepod copepodites, excluding *Oncaea* sp. of Poecilostomatoid copepods, collected with the van-Dorn bottle were standardized by filtered volume (6.8 L) and expressed as prey density (inds./L) because *Oncaea* sp. copepodites were infrequent in the digestive tracts of *P. azonus* larvae (see Results section).

Data on the content of the digestive tract were expressed as percentage occurrence frequency (%F, representing the percentage of larvae that consumed a particular type of prey), as well as by number and volume percentage (%N and %V, indicating the percentage of each prey type in relation to the total number and volume of prey items, respectively). The %IRI for prey type *i* was calculated as a percentage of index of relative importance (IRI; Pinkas et al. 1971) using Eq. 4 and Eq. 5:

$$\%IRI_i = IRI_i \cdot 100/\sum IRI \tag{4}$$

$$IRI_i = (\%N_i + \%V_i) \cdot \%F_i \tag{5}$$

The feeding rate was determined (%FR; the proportion of larvae having prey in the digestive system to the total number of larvae tested). Mean feeding intensities (FIinds (individuals/larva) [Eq. 6] and FIvol (mm$^3$/larva) [Eq. 7]) were calculated for each sampling station, and median values were calculated for feeding intensities by larval developmental stage and sampling day, including specimens with small sample sizes. These feeding intensity estimates, however, excluded *Oncaea* sp. copepodites.

$$FIinds = prey\,number\,of\,individuals/larva \tag{6}$$

$$FIvol = prey\,volume/larva \tag{7}$$

Tukey–Kramer multiple comparison tests were used to compare weighted mean depths (WMD from Eq. 2),

arcsine-transformed relative weighted mean depth (RWMD from Eq. 3), and log(x + 1)-transformed prey density in the four major periods across sample regions (A, B, C, and D). The *G*-test was used to compare the composition of prey items in the larval diet (%*N*) among sample locations, and the Kruskal–Wallis test with order was used to compare the composition of larval developmental stages between the 0-m and 10-m depth layers. The *U*-test was employed between two groups for water temperature, salinity, prey density, larval NL, and feeding intensity, while Steel–Dwass and Scheffe's multiple comparison tests were utilized between ≥ 3 groups. The Shirley-Williams multiple comparison test was used to compare SLL samples of neighboring ordinals of ≥ 3. The significance level was set to 0.05.

The maximum likelihood technique was used to analyze the interaction between abiotic and biotic variables for feeding intensities for *P. azonus* larvae at 37 sample locations over the four major periods using IBM SPSS AMOS version 26 (IBM Corp., Armonk, NY, USA). Exogenous variables included sea surface temperature and salinity, bottom depth at each sampling station, and sampling time. Endogenous variables included NL of *P. azonus* larvae, log(x + 1)-transformed density of copepod copepodites excluding *Oncaea* sp., log(x + 1)-transformed mean feeding intensity by prey individuals (mean FIinds from Eq. 6), and log(x + 0.001)-transformed mean feeding intensity by prey volume (mean FIvol from Eq. 7). Path analysis approaches enable researchers to assess the fit of the correlation matrix against ≥ 2 causal models, eliminating the requirement for often misleading univariate studies. Goodness-of-fit measures [e.g., $R^2$ for endogenous variables, the goodness of fit index (*GFI*), the adjusted good of fit index (*AGFI*), and the root mean square of approximation (*RMSEA*)] were used to choose path models (i.e., whether indirect paths between nonneighboring factors are inclusive or not). For the comparison of log(x + 1)-transformed mean FIinds across sample regions, one-way analysis of variance (*ANOVA*) was utilized.

## Results

### Seasonal changes in oceanographic conditions

The median surface water temperature in the research region across the 3 years covering the 3 year-classes of *P. azonus* ranged from 12.8 °C to 15.8 °C in November to 6.6 °C to 7.9 °C in February (Table 1). Sea surface salinity was highest in January–February (median 33.87–34.03), with the exception of the 27 November 2008 survey (34.04). The salinity was lower in November 2010–February 2011 (33.61–33.91) than in the previous 2 years (33.84–34.04). During all survey periods, coastal sampling stations in the B, C, and D regions had lower temperatures and salinities than offshore stations,

while those in the A region did not show a consistent trend between coastal and offshore stations (Fig. 3).

### Comparison of densities of *P. azonus* larvae at the surface and 10-m-depth layers

The surface-specific occurrence of *P. azonus* larvae along the Tatehama coast in Tsugaru Strait was similar to the results from collections in the Sado Strait (Okiyama 1965). *Pleurogrammus azonus* larvae were collected from the large yolk-sac stage through the flexion stage; however, no postflexion larvae were sampled in this investigation. Because very substantial numbers of *P. azonus* larvae were collected at five stations (Stns. N30, W40, I60, F60, and T80) on 28–29 January 2009 and one station (Stn. T50) on 18 February 2010, we compared the median larval densities of the 0-m and 10-m depth layers of these six stations. The median density was significantly greater in the 0-m-depth layer than in the 10-m-depth layer (Eq. 1; 14.17 vs. 1.94 inds./1000 m$^3$, respectively; *U*-test, *p* = 0.010). The median NLs of larvae taken in both strata were not significantly different (*U*-test, *p* = 0.12; 9.08 mm NL [*n* = 39] at 0 m and 9.84 mm NL [*n* = 5] at 10 m). There was no significant difference in the composition of the developmental stages (Kruskal–Wallis test with order, *p* = 0.50), and small yolk-sac stage larvae (0 m: 54%, 10 m: 20%) and preflexion larvae (0 m: 33%, 10 m: 60%) were abundant in both strata.

### Temporal and horizontal changes in distribution of *P. azonus* larvae and their prey at the surface layer

*Pleurogrammus azonus* larvae were mostly sampled in the 0-m-depth layer on 21 and 28–29 January 2009, 18–19 February 2010, 27–28 January 2011, and 14–15 February 2011 (Table 1); however, they were barely sampled in November and December. Larvae were collected at temperatures ranging from 6.50 °C (minimum) to 8.70 °C (median) to 12.30 °C (maximum) (minimum-median-maximum; *n* = 71) and salinities ranging from 32.36 to 33.94 to 34.10 (minimum-median-maximum). The highest densities were observed at Stn. T20 near Tatehama in region A at three different times (596 inds./1000 m$^3$ in 18–19 February 2010; 1850 inds./1000 m$^3$ in 27–28 January 2011; 47.9 inds./1000 m$^3$ in 14–15 February 2011; Fig. 3). Higher densities were observed at Stn. F20 and Stn. F60 off Fukushima in region B on 21 and 28–29 January 2009 (80.6 inds./1000 m$^3$ and 79.1 inds./1000 m$^3$, respectively), and at Stn. TM10 in region A (69.0 inds./1000 m$^3$). There were no larvae collected at Stn. N10, which is situated in the inner C region, or at Stn. H20, which is located in the inner D region. The mean density was significantly higher in region A than in the other three regions (89.6
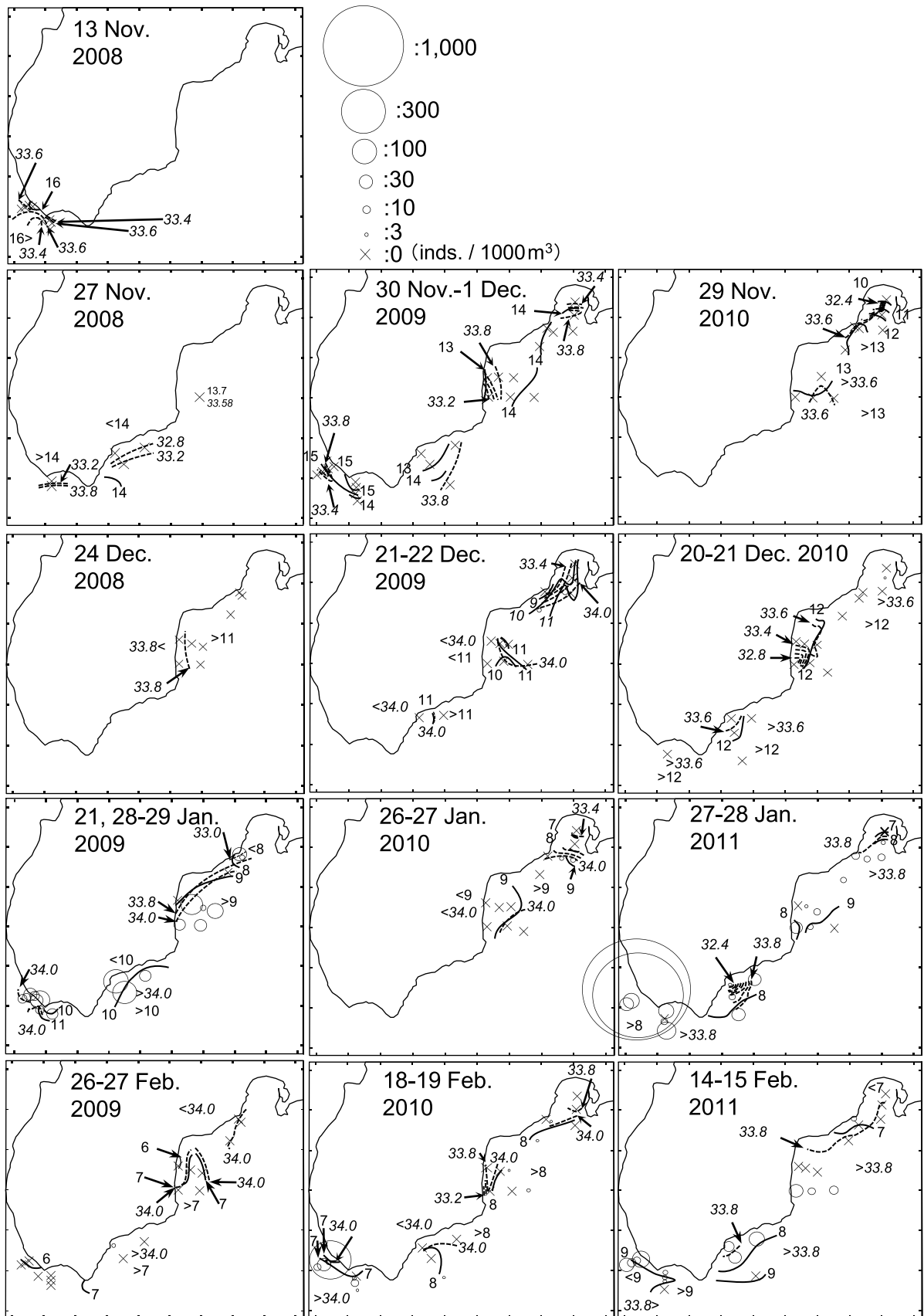
vs. 0.68–1.13 inds./1000 m$^3$, respectively) in February 2010, and the mean density in region A was higher than that in regions C and D in January 2011 (472.1 vs. 6.2 and 5.3 inds./1000 m$^3$, respectively) (both comparisons by the Tukey–Kramer multiple comparison test, both $p < 0.05$; Fig. 4).

The weighted mean depths (WMD from Eq. 2) obtained from *P. azonus* larval densities at surface layers and seabed depths of sampling stations were compared by sampling region. The mean WMD in region B (68.7 m) was significantly deeper than that of regions C and D (32.1 and 27.5 m, respectively; Tukey–Kramer multiple comparison test, both $p < 0.05$; Table 2). The mean value of relative weighted mean depth (RWMD from Eq. 3) in region B (79%) was significantly higher than in region A (42%; $p < 0.05$; Table 2). According to these findings, *P. azonus* larvae were more abundant at the coastal stations in region A and offshore in region B.

Almost all large yolk-sac stage larvae (95.5%) were obtained in region A, with the remainder collected in regions B (Stn. F60: 0.6%), C (W10, W40, N20, and N40: 2.8%), and D (D30: 1.1%; Fig. 4). Flexion-stage larvae, the most developed larvae collected in this study, were recorded only in regions B, C, and D. There was a significant difference in median NLs by developmental stage (Kruskal–Wallis test with order, $p < 0.001$; large yolk-sac-stage larvae: 7.9–9.0–9.9 mm; middle yolk-sac: 7.9–9.2–10.7 mm; small yolk-sac: 7.4–9.3–10.6 mm; preflexion: 7.4–9.9–12.9 mm; and flexion: 10.3–12.6–13.9 mm, as minimum-median-maximum NL).

Across the four major survey periods, the mean density of copepod copepodites excluding *Oncaea* sp. was significantly higher in region A than in region C (2.7 vs. 1.5 inds./L, respectively; Tukey–Kramer multiple comparison test, $p < 0.05$; Table 2). During these four major periods, *O. similis* copepodites was found to account for the highest proportion (41–64% in range of all copepodites excluding *Oncaea* sp.).

### Diet composition and feeding intensity of *P. azonus* larvae

For *P. azonus* larvae at the large yolk-sac stage to the preflexion stage, cyclopoid copepodites occupied a large part of the diet (%$F$ = 52–98; %$IRI$ = 61.7–73.3 [Eq. 4]; Table 3), in particular, middle-sized cyclopoid *Oithona similis* in the copepodite stage (%$F$ = 43–96; %$IRI$ = 51.1–71.3). Small-sized species of *O. oculata* copepodites were frequently

preyed on by *P. azonus* larvae but represented small %$IRI$ (%$F$ = 29–71; %$IRI$ = 1.7–7.9). Large-sized species of *Oithona* spp. (*O. atlantica*, *O. longispina*, and *O. plumifera*) copepodites were occasionally preyed upon by *P. azonus* larvae but also represented small %$IRI$ from the large yolk-sac stage to the preflexion stage (shown as *Oithona* spp. combined: %$F$ = 11–30; %$IRI$ = 0.3–2.4). Copepods in the nauplius stage were the second-most dominant prey from the large yolk-sac stage to the preflexion stage (%$F$ = 38–75; %$IRI$ = 15.2–24.4). Poecilostomatoid *Oncaea* sp. in the copepodite stage was only rarely found in the diet (%$F$ = 0–12; %$IRI$ = 0–0.1).

Analysis of four flexion-stage larvae of *P. azonus* revealed that they chiefly preyed on calanoid copepods in the copepodite stage (%$F$ = 100; %$IRI$ = 84.1), especially *Clausocalanus* sp. (%$F$ = 100; %$IRI$ = 69.4) and *Pseudocalanus newmani* (%$F$ = 50; %$IRI$ = 10.9). *Oithona similis* copepodites were the second-most dominant prey (%$F$ = 75; %$IRI$ = 13.4).

At the genus or species level, copepod nauplii ($n = 418$) were identified in the diet of *P. azonus* larvae ($n = 228$) throughout all larval stages collected on 27–28 January 2011. The composition of the diet of the different copepod nauplii in terms of number and volume was 51.0% and 33.2% for *O. similis*, 7.9% and 14.8% for *P. newmani*, 0.5% and 0.2% for *Paracalanus* and *Clausocalanus* spp., 0.5% and 0.1% for *Oncaea* sp., 21.5% and 35.1% for unidentifiable calanoid nauplii by digestion, and 18.7% and 16.6% for unidentifiable copepod nauplii, respectively.

Median feeding intensities by number of prey individuals (median FIinds [Eq. 6]) increased from 3 inds./larva in the large yolk-sac stage to 20.5 inds./larva in the preflexion stage; however, the number slightly decreased in the flexion stage (17 inds./larva; Table 3). Median feeding intensities by prey volume (median FIvol [Eq. 7]) increased from 0.007 mm$^3$/larva in the large yolk-sac stage to 0.199 mm$^3$/larva in the flexion stage. The percentage of empty digestive tracts decreased with growth, from 24% in the large yolk-sac stage to 0% in the preflexion or flexion stages.

Geographical changes in diet compositions (%$N$ and %$V$) and median feeding intensities (median FIinds and FIvol) were examined in preflexion-stage larvae that were widely distributed across the four sampling regions. Major prey composition in terms of %$N$ was significantly different among the sampling regions (G-test, $p < 0.001$; Fig. 5). *Oithona similis* copepodite was the most common prey item in all four regions in terms of %$N$ (35.0–42.9%) and in regions A, B, and D in terms of %$V$ (32.1–46.0%). The %$V$ of *P. orientalis* copepodite was slightly higher than that of *O. similis* copepodite (21.7% vs. 20.0%, respectively) in region C. Median feeding intensities significantly differed among regions by the Steel–Dwass test at the 0.05 significance level, with those in region C (median FIinds = 11 inds./
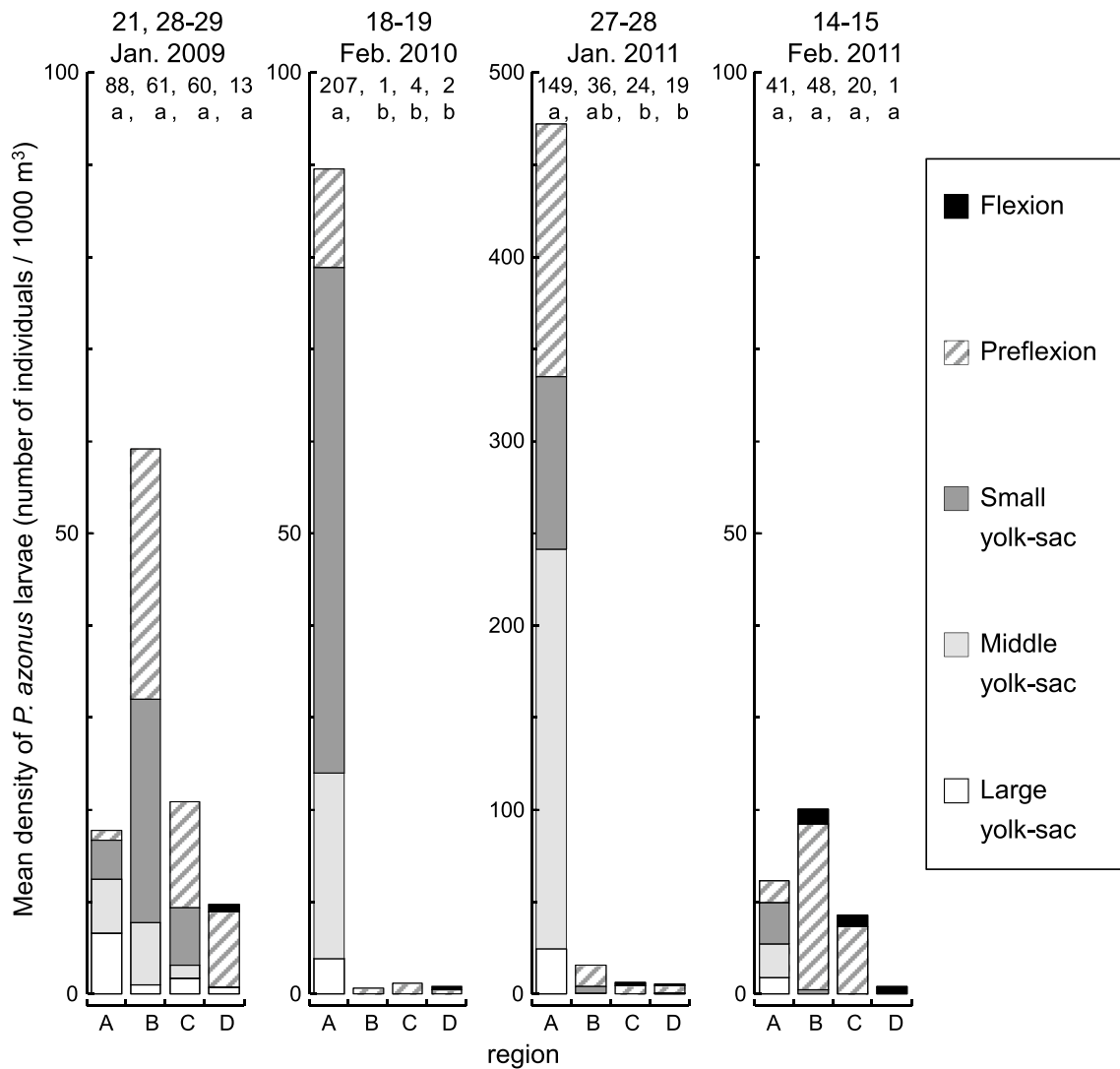
**Fig. 4** Mean density of *P. azonus* larvae (number of individuals/1000 m³) by region by developmental stage. The numbers above the bars indicate the sample size

**Table 2** Mean bottom depth of sampling stations weighted by the densities of *Pleurogrammus azonus* larvae, relative bottom depth to maximum bottom depth where *P. azonus* larvae were collected, and mean prey density, by sampling region across the four major periods (21 and 28–29 January 2009, 18–19 February, 2010, 27–28 January 2011, and 14–15 February 2011)

| Measures | Region | | | |
| --- | --- | --- | --- | --- |
| | A | B | C | D |
| WMD (m)[a] | 45.4a,b | 68.7a | 32.1b | 27.5b |
| RWMD (%)[b] | 42b | 79a | 58a,b | 45a,b |
| Prey density (inds./L)[c] | 2.7 ± 1.64a | 2.2 ± 0.86a,b | 1.5 ± 1.15b | 1.7 ± 0.97a,b |

Different letters indicate significant differences in WMD, arcsine-transformed RWMD, and log($x$ + 1)-transformed prey density at $p \leq 0.05$ by Tukey–Kramer multiple comparison test

[a]WMD is the weighted mean bottom-depth of sampling stations (from Eq. 2)

[b]RWMD is relative bottom-depth to the maximum bottom-depth where *P. azonus* larvae were collected (from Eq. 3)

[c]Mean prey density (± standard deviation) included copepod nauplii and copepodites and excluded *Oncaea* sp. copepodites

**Table 3** Composition of the diet of *Pleurogrammus azonus* larvae across different developmental stages

| Taxa | Large yolk-sac stage | | | | Middle yolk-sac stage | | | | Small yolk-sac stage | | | | Preflexion stage | | | | Flexion stage | | | |
|---|---|---|---|---|---|---|---|---|---|---|---|---|---|---|---|---|---|---|---|---|
| | %F | %N | %V | %IRI | %F | %N | %V | %IRI | %F | %N | %V | %IRI | %F | %N | %V | %IRI | %F | %N | %V | %IRI |
| *Noctiluca* sp. | 0 | 0 | 0 | 0 | 0 | 0 | 0 | 0 | 1 | <0.1 | 0.1 | <0.1 | 0 | 0 | 0 | 0 | 0 | 0 | 0 | 0 |
| Rotatoria *Trichocerca marina* | 0 | 0 | 0 | 0 | 0 | 0 | 0 | 0 | 1 | <0.1 | <0.1 | <0.1 | 0 | 0 | 0 | 0 | 0 | 0 | 0 | 0 |
| Copepoda (copepodite; total) | 62 | 72.6 | 84.9 | 75.6 | 91 | 69.4 | 83.1 | 81.3 | 93 | 68.4 | 80.8 | 77.2 | 100 | 73.6 | 83.1 | 82.0 | 100 | 93 | 99.1 | 99.4 |
| Calanoida (copepodite; total) | 38 | 10.7 | 22.7 | 8.5 | 64 | 10.9 | 22.3 | 7.6 | 67 | 7.5 | 14.7 | 4.8 | 80 | 17.2 | 37.7 | 19.5 | 100 | 68 | 89.0 | 84.1 |
| *Calanus pacificus* | 0 | 0 | 0 | 0 | 0 | 0 | 0 | 0 | 0 | 0 | 0 | 0 | 1 | <0.1 | 0.1 | <0.1 | 0 | 0 | 0 | 0 |
| *Mesocalanus tenuicornis* | 0 | 0 | 0 | 0 | 2 | 0.2 | 0.2 | <0.1 | 2 | 0.1 | 0.1 | <0.1 | 2 | 0.1 | 0.2 | <0.1 | 0 | 0 | 0 | 0 |
| *Eucalanus* sp. | 0 | 0 | 0 | 0 | 0 | 0 | 0 | 0 | 0 | 0 | 0 | 0 | 1 | <0.1 | 0.1 | <0.1 | 0 | 0 | 0 | 0 |
| *Paracalanus orientalis* | 14 | 4.8 | 5.7 | 2.3 | 18 | 2.6 | 4.0 | 1.0 | 27 | 2.1 | 5.0 | 1.3 | 53 | 6.8 | 16.9 | 9.0 | 25 | 3 | 4.1 | 1.1 |
| *Clausocalanus* sp. | 5 | 1.2 | 1.4 | 0.2 | 18 | 2.1 | 2.4 | 0.7 | 36 | 2.1 | 3.3 | 1.3 | 55 | 4.1 | 7.7 | 4.7 | 100 | 47 | 61.2 | 69.4 |
| *Pseudocalanus newmani* | 19 | 4.8 | 15.6 | 6.0 | 36 | 5.7 | 14.0 | 5.9 | 41 | 2.6 | 4.6 | 2.1 | 52 | 4.0 | 9.8 | 5.1 | 50 | 15 | 18.7 | 10.9 |
| *Pseudocalanus minutus* | 0 | 0 | 0 | 0 | 0 | 0 | 0 | 0 | 0 | 0 | 0 | 0 | 2 | 0.1 | 0.2 | <0.1 | 50 | 3 | 4.8 | 2.4 |
| *Paraeuchaeta* sp. | 0 | 0 | 0 | 0 | 2 | 0.2 | 1.2 | <0.1 | 4 | 0.2 | 1.1 | <0.1 | 1 | <0.1 | 0.1 | <0.1 | 0 | 0 | 0 | 0 |
| *Scolecithricella minor* | 0 | 0 | 0 | 0 | 2 | 0.2 | 0.4 | <0.1 | 1 | <0.1 | 0.2 | <0.1 | 3 | 0.1 | 0.3 | <0.1 | 0 | 0 | 0 | 0 |
| Unidentified calanoid copepodites | 0 | 0 | 0 | 0 | 0 | 0 | 0 | 0 | 6 | 0.3 | 0.4 | <0.1 | 24 | 1.8 | 2.5 | 0.8 | 25 | 1 | 0.1 | 0.2 |
| Cyclopoida (copepodite; total) | 52 | 54.8 | 54.8 | 61.7 | 82 | 56.6 | 59.3 | 73.3 | 93 | 59.7 | 64.4 | 72.1 | 98 | 54.5 | 43.4 | 61.7 | 75 | 23 | 9.3 | 15.0 |
| *Oithona* spp.[a] | 14 | 4.8 | 6.3 | 2.4 | 11 | 1.2 | 2.1 | 0.3 | 23 | 1.1 | 2.0 | 0.5 | 30 | 1.5 | 1.9 | 0.7 | 0 | 0 | 0 | 0 |
| *Oithona similis* | 43 | 36.9 | 39.9 | 51.1 | 82 | 51.1 | 55.0 | 71.3 | 89 | 52.2 | 59.0 | 68.8 | 96 | 40.8 | 36.7 | 53.0 | 75 | 19 | 8.6 | 13.4 |
| *Oithona davisae* | 5 | 1.2 | 1.0 | 0.2 | 2 | 0.2 | 0.2 | <0.1 | 7 | 0.3 | 0.3 | <0.1 | 3 | 0.1 | 0.1 | <0.1 | 0 | 0 | 0 | 0 |
| *Oithona oculata* | 29 | 10.7 | 7.1 | 7.9 | 34 | 4.0 | 1.9 | 1.7 | 49 | 5.1 | 2.7 | 2.7 | 71 | 11.3 | 4.3 | 7.9 | 50 | 4 | 0.6 | 1.5 |
| Unidentified *Oithona* spp. | 5 | 1.2 | 0.6 | 0.1 | 2 | 0.2 | 0.1 | <0.1 | 9 | 0.9 | 0.5 | 0.1 | 16 | 0.7 | 0.4 | 0.1 | 0 | 0 | 0 | 0 |
| Poecilostomatoida *Oncaea* sp. | 0 | 0 | 0 | 0 | 5 | 0.3 | 0.4 | <0.1 | 4 | 0.1 | <0.1 | <0.1 | 12 | 0.6 | 0.2 | 0.1 | 0 | 0 | 0 | 0 |
| Unidentified copepodites | 24 | 7.1 | 7.4 | 5.4 | 18 | 1.6 | 1.2 | 0.4 | 19 | 1.1 | 1.6 | 0.3 | 29 | 1.4 | 1.9 | 0.7 | 25 | 1 | 0.9 | 0.4 |
| Copepoda (nauplius) | 38 | 26.2 | 15.1 | 24.4 | 57 | 26.4 | 12.1 | 18.0 | 75 | 26.9 | 12.9 | 20.9 | 73 | 20.4 | 8.7 | 15.2 | 25 | 3 | 0.9 | 0.6 |
| Appendicularia *Oikopleura* sp. | 0 | 0 | 0 | 0 | 14 | 1.7 | 4.5 | 0.7 | 31 | 2.8 | 5.9 | 1.9 | 34 | 2.9 | 7.9 | 2.6 | 0 | 0 | 0 | 0 |
| Gastropoda (larva) | 0 | 0 | 0 | 0 | 0 | 0 | 0 | 0 | 0 | 0 | 0 | 0 | 2 | 0.1 | <0.1 | <0.1 | 0 | 0 | 0 | 0 |
| Invertebrates (egg) | 0 | 0 | 0 | 0 | 5 | 0.3 | 0.2 | <0.1 | 10 | 0.5 | 0.2 | <0.1 | 10 | 1.8 | 0.2 | 0.1 | 0 | 0 | 0 | 0 |
| Unidentified particle | 5 | 1.2 | – | – | 18 | 2.1 | – | – | 21 | 1.4 | – | – | 18 | 1.2 | – | – | 25 | 4 | – | – |
| Min.-me.-max. FIinds (inds./larva)[b] | 0–3–18 | | | | 0–8–69 | | | | 0–20–96 | | | | 2–20.5–83 | | | | 16–17–23 | | | |
| Min.-me.-max. FIvol (mm³/larva)[b] | 0–0.007–0.036 | | | | 0–0.030–0.258 | | | | 0–0.079–0.304 | | | | 0.006–0.091–0.360 | | | | 0.086–0.199–0.247 | | | |
| Number of larvae examined and empty guts (%FR) | 21/5 (24%) | | | | 44/5 (11%) | | | | 81/6 (7%) | | | | 94/0 (0%) | | | | 4/0 (0%) | | | |

*%F* Percentage of larvae that consumed a particular type of prey (expressed as percentage occurrence frequency), *%N* percentage of each prey type in relation to the total number, *%V* percentage of prey items in relation to total volume, *%IRI* percentage of index of relative importance

[a] *Oithona atlantica*, *O. longispina*, and *O. plumifera*

[b] Minimum-median-maximum, FIinds feeding intensity by prey individuals from Eq. 6 and FIvol feeding intensity by prey volume from Eq. 7 in the text
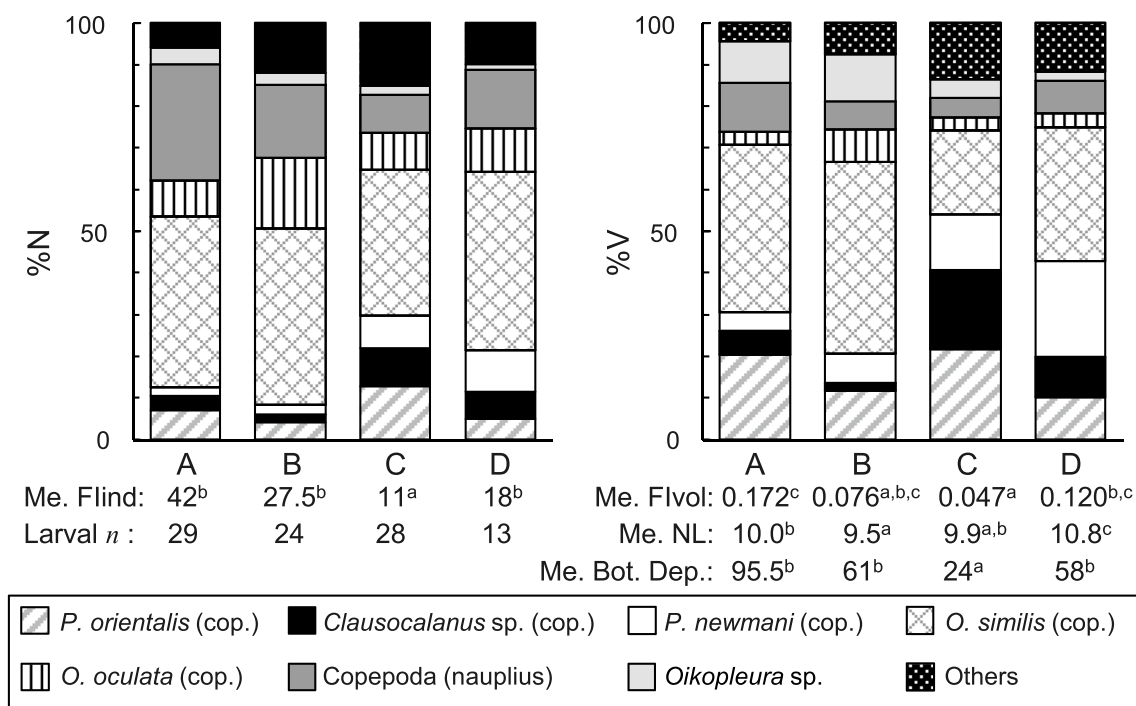
**Fig. 5** Major prey compositions of *P. azonus* preflexion larvae in terms of %N and %V (the percentage of each prey type in relation to the total number and volume of prey items, respectively) by sampling region. Medians of feeding intensities in terms of number and volume (FIinds by inds./larva and FIvol by mm³/larva, respectively), sample larva; FIvol = 0.047 mm³/larva) having the lowest values. In region C, the median NL of preflexion larvae whose diet sizes of larval diet examined, median NL (notochord length) of larvae examined (mm), and median sea-bottom depth (Me. Bot. Dep.) where larvae were collected (m) are noted. Different letters (superscripts) indicate significant differences within medians

larva; FIvol = 0.047 mm³/larva) having the lowest values. In region C, the median NL of preflexion larvae whose diet compositions were examined was intermediate (9.9 mm NL) between the four regions, and the median sea-bottom depth where preflexion larvae were collected was the shallowest (depth: 24 m).

The median second-largest lengths (SLLs) of prey items in the digestive tracts of *P. azonus* larvae gradually increased within the same taxonomic group with larval development; however, median SLLs showed insignificant differences in *O. oculata* copepodites, three large-sized *Oithona* spp. copepodites, and *Oikopleura* sp. (Fig. 6). The differences in median SLL were smaller in copepod nauplii and cyclopoid copepodites than in calanoid copepodites, reflecting the larger size and wider range of calanoid SLLs.

### Interaction between feeding intensities of *P. azonus* larvae and environmental factors

The effects of NL of *P. azonus* larvae from the large yolk-sac to preflexion stages, environmental factors, and day-time sampling time on mean larval mean feeding intensities (mean FIinds and mean FIvol) of 37 sampling stations ($n = 37$) in four major periods were evaluated using path analysis (Fig. 7). We detected geographic differences between median FIinds using data only from preflexion-stage larvae (Fig. 5). However, this path analysis used larvae from a wide range of developmental stages and there was no significant difference in $\log(x + 1)$-transformed mean FIinds across regions (*ANOVA, p = 0.25*), so sampling location data were removed from the path analysis as exogenous or endogenous variables. Sea surface temperature, sea-bottom depth, and larval NL explained 52% of variance in mean FIinds ($R^2 = 0.52$). Mean FIinds increased with increasing sea-bottom depth ($\beta = 0.47$, $p < 0.001$; Fig. 7), and no low mean FIinds were recorded in deep sampling stations in regions A and B (Electronic Supplementary Material [ESM] Fig. S1a). Mean FIinds rose ontogenetically, and this increased with larval NL ($\beta = 0.33$, $p = 0.020$; ESM Fig. S1c). In conditions of low water temperature, mean FIinds were high ($\beta = -0.41$, $p = 0.002$; Fig. S1b). There were two negative indirect effects of water temperature: via larval NL ($\beta = -0.48 \times 0.33 = -0.16$) and via sea-bottom depth through larval NL ($\beta = -0.34 \times 0.33 = -0.11$; Fig. 7); however, these effects were minor compared to the direct effects. Larvae with greater mean FIinds had higher mean FIvol ($\beta = 0.82$, $p < 0.001$; Fig. 7; ESM Fig. S1h), and mean FIvol rose with increasing larval NL ($\beta = 0.31$, $p < 0.001$; Fig. 7; ESM Fig. S1g). Both effects explained
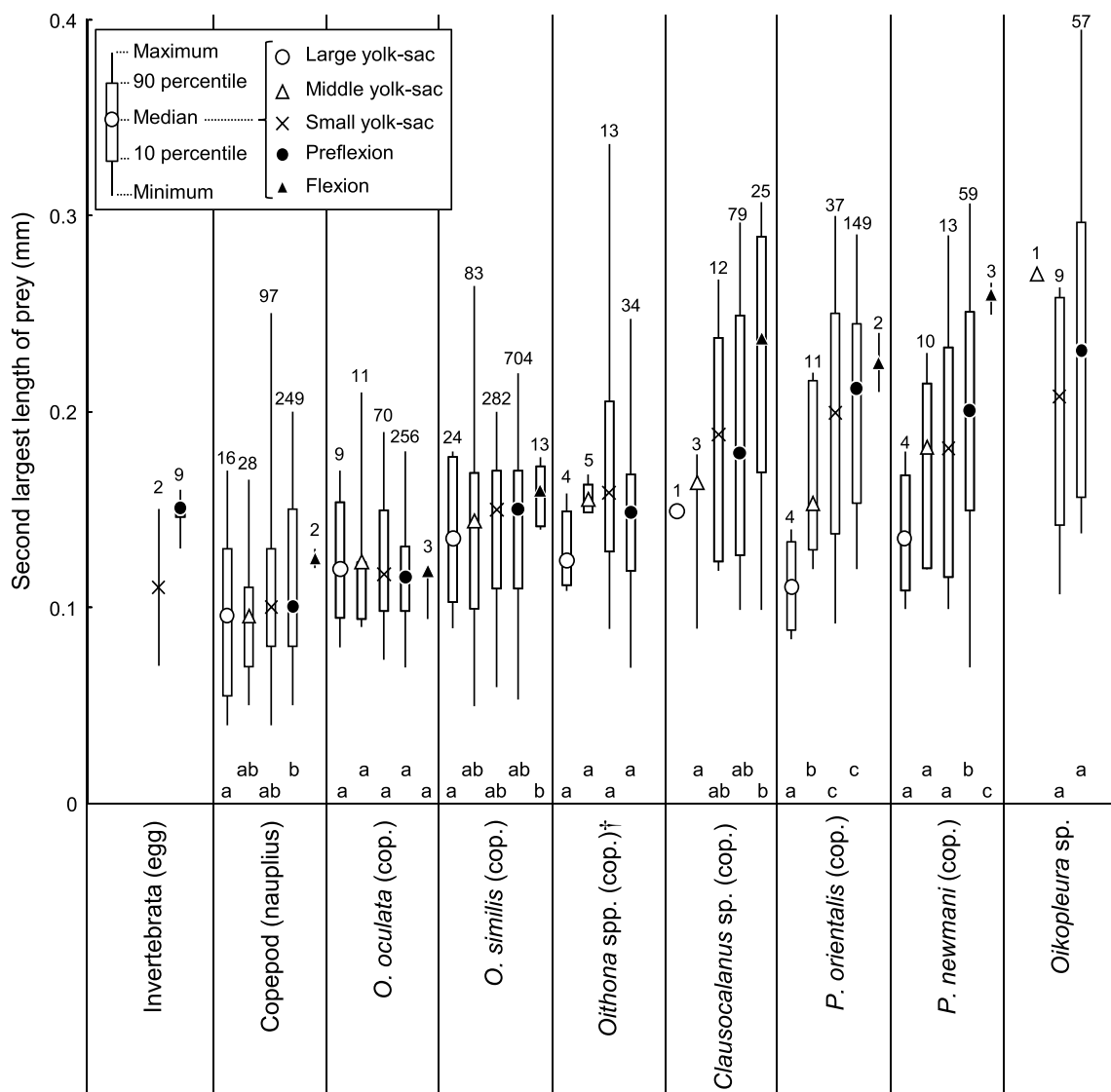
**Fig. 6** Prey-size (second-largest length [SLL]) differences in larval *P. azonus* diet by developmental stage. Dagger (†) following *Oithona* spp. includes three large-sized species: *O. atlantica*, *O. longispina*, and *O. plumifera*. Different letters indicate significant differences at $p < 0.05$ in the same prey item by the Mann–Whitney $U$-test between two samples and by the Shirley-Williams test between two adjacent ordinal samples. These statistical tests were performed between samples ($n \geq 3$). Superscripts indicate sample sizes ($n$). *cop.* Copepodite

95% of the variance ($R^2 = 0.95$; Fig. 7). The former had a 2.6-fold bigger impact than the latter ($= 0.82/0.31$), demonstrating that *P. azonus* larvae preferred feeding on multiple prey individuals rather than changing to larger-sized prey when body size increased from the large yolk-sac stage to the preflexion stage. There was no significant interaction between mean FIinds and prey density (cope-podites excluding *Oncaea* sp.; ESM Fig. S1d). The effect of surface salinity was insignificant to the mean FIinds and mean FIvol of *P. azonus* larvae. Because larvae were collected at shallower sampling stations early in the daytime and at deeper depth stations in the late daytime in this study, sampling time had a significant positive correlation

with sea bottom depth at sampling stations ($r = 0.46$, $p = 0.012$); however, the sampling time had no direct effects on any endogenous variables, including two feeding intensities.

## Discussion

Almost all large yolk-sac stage larvae of *P. azonus* were predominantly found in the surface layer near the Tate-hama coast in the spawning ground of region A during late January to late February, and flexion-stage larvae, the most developed larvae, were recorded only in regions B, C, and
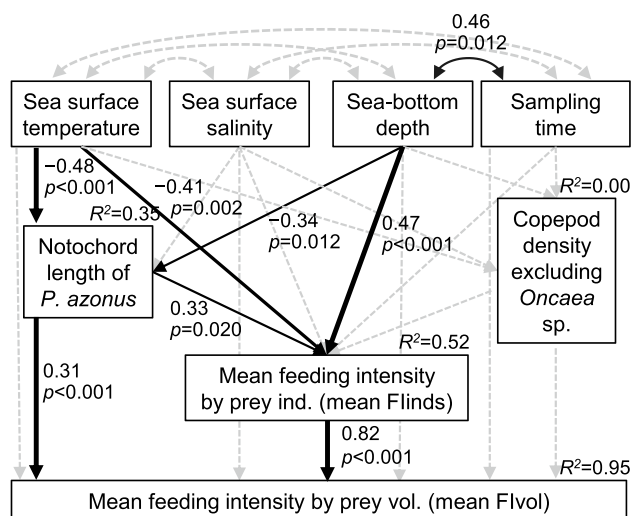
**Fig. 7** Path model of the interaction between mean feeding intensity by prey individuals and volume of copepodites excluding *Oncaea* sp. at each sampling station and under different environmental factors of *P. azonus* larvae around Matsumae Peninsula during four sampling periods (21 and 28–29 January 2009, 18–19 February 2010, 27–28 January 2011, and 14–15 February 2011) ($\chi^2 = 25.73$, $n = 37$, $df = 20$, $GFI = 0.852$, $AGFI = 0.734$, $CFI = 0.963$, and $RMSEA = 0.089$). Numbers above the two-direction curved arrows indicate correlation coefficients ($r$) between exogenous variables. Numbers alongside single straight arrows indicate the standardized path coefficients ($\beta$). Numbers above the boxes represent the squared multiple correlations ($R^2$). Gray, broken arrows between parameters indicate no significance between those parameters ($p \geq 0.05$). *AGFI* Adjusted goodness of fit index, *CFI* comparative fit index, *GFI* goodness of fit index, *RMSEA* root mean square error of approximation

D (Figs. 3, 4). In addition, the WMD and the RWMD in region B were the highest across all regions (Table 3). *Pleurogrammus azonus* larvae were estimated to be transported offshore from the spawning ground by branches of the TsWC and the TgWC (Fig. 8). Larvae would successfully increase their feeding intensities by being transported offshore, thus obtaining a favorable environment for survival in the Tsugaru Strait. In the Tsugaru Strait, the sea level in the Japan Sea at the western entrance of the strait is higher than that in the Pacific Ocean at the eastern entrance, resulting in an eastward flow (Toba et al. 1982). The highest current velocity was found to be offshore of Cape Shirakami (Fig. 1) at the boundary of regions A and B, due to the narrowest distance from the opposite shore in Tsugaru Strait (Odamaki 1985). On the other hand, the water of the coastal areas of regions B, C, and D have a lower surface salinity (Fig. 3) and a slower velocity than the central part of the Tsugaru Strait (Odamaki 1985). Therefore, *P. azonus* spawning off Tatehama probably successfully reproduce by taking advantage of the unique topography and current system at the western mouth of the Tsugaru Strait.

The variable that influenced the mean feeding intensity by prey individuals (mean FIinds) on larvae by sampling station

was the sea-bottom depth, with deeper stations having higher FIinds (Fig. 7; ESM Fig. S1a). However, there was no interaction between mean FIinds and prey density (Fig. 7; ESM Fig. S1d), and the prey density in the offshore surface layer was not often higher than that in the coastal layer within the sampling regions where larvae were collected. This finding might reflect the lower density of copepods in surface water in the daytime compared to the deeper layers. The offshore surface layers would be more readily supplied with prey copepods from the deeper layers in the nighttime by diurnal vertical migration, whereas the coastal surface layers were not supplied with prey copepods other than by horizontal transport. Although we did not examine the vertical distribution of copepods in this study, for example, all life stages of *O. similis* were relatively scarce in the top few meters of the water column, and napulii, copepodites; in addition, adult stages of this prey species were found to be abundant at depths of 10, 10–25 m, and ≥ 25 m off the UK at mid-morning (Cornwell et al. 2020). The spawning grounds of *P. azonus* are on open coastal areas rather than in inner bays (Kambara 1957), and the Tatehama coast may have been selected as one of the spawning grounds for adults because of its short distance to offshore areas favorable for larva feeding, which may help stabilize feeding success during the initial feeding period.

The biology and morphology of fat greenling *Hexagrammos otakii* larvae are similar to those of *P. azonus* (Joh et al. 2008). In the present study, *H. otakii* larvae were collected with *P. azonus* larvae mostly in regions C and D (E. Ooka, unpublished data, 2012). The shorelines in regions C and D are somewhat confined, and the distances to offshore deep-water zones are longer than those in the A and B regions (Fig. 8). The prey species of *H. otakii* is comparable to that of *P. azonus* in the Sea of Japan (Davydova et al. 2007). *Pleurogrammus azonus* larvae and juveniles live a pelagic life until about 10 months after hatching and they use the extensive offshore areas as a nursery area (Kyushin 1977; Davydova et al. 2007), whereas *H. otakii* larvae live a pelagic life for about 40 days and juveniles settle on the coast (Fukuhara and Fushimi 1983; Joh et al. 2008). As a result, the varying distances between spawning grounds and continental shelf slope waters may be attributable to differences in access to nursery areas during the juvenile stages.

Hexagrammidae larvae, including *P. azonus* and *H. otakii*, exhibit well-developed morphologies upon hatching as compared to larvae of other families that begin feeding on copepod nauplii. Hexagrammid larvae have bigger egg diameters (≥ 1.5 mm), longer hatching body lengths (6.5–9.9 mm), large eyes with guanine pigmentation, coiled digestive tracts, and heavy body pigmentation (Nagasawa and Saito 2014). Such morphologies would allow for feeding on copepodites from the beginning of the feeding stage, and their feeding intensity would be less likely to diminish
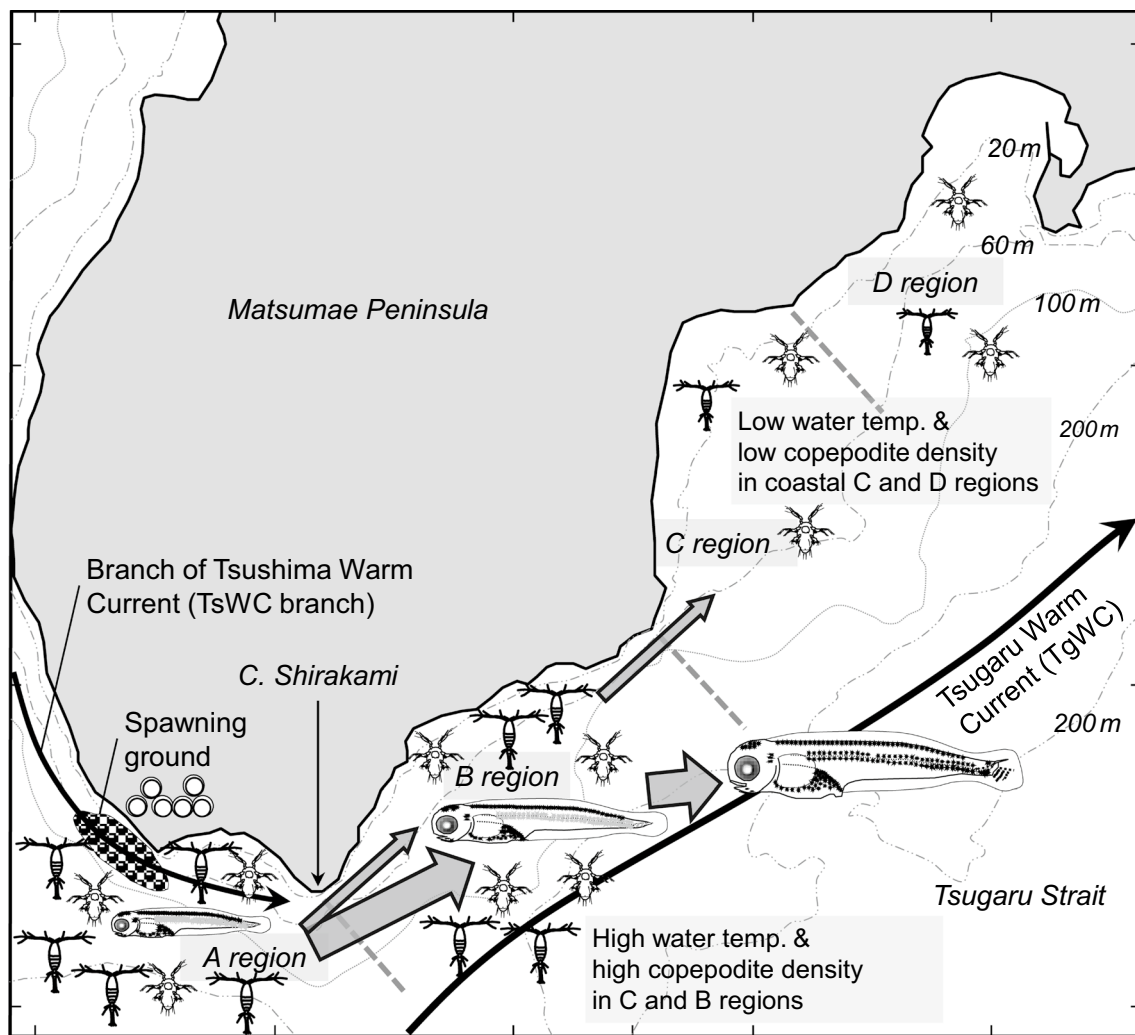
**Fig. 8** Schematic diagram of the spatial distribution of *P. azonus* larvae in the abiotic and biotic environments around the Matsumae Peninsula. The gray arrows indicate the direction in which the larvae are transported, and the width of the arrows indicates the abundance of the larvae being transported. The number of copepods in each region indicates the abundance of prey species

if they started from copepod nauplii. The optimal feeding environment for the development of omnivorous fishes is a gradual increase in the body size of the respective prey as the fish grows; however, the size spectrum of prey in wild environments is usually discontinuous, and feeding intensities of larvae and juveniles frequently decrease during the prey shift period in environments with fewer larger sized prey (Takatsu et al. 1995; Takatsu 1998). Prey changes in accordance with huge gaps in prey body size may be one of the reasons for growth stagnation, resulting in decreased survival, particularly for larval and juvenile fish, which are sluggish swimmers with a limited range for searching for prey (Takatsu 1998). We observed that feeding intensities were greater in bigger-sized *P. azonus* larvae (Fig. 7), most likely due the ability of larger individuals to swim faster (Faillettaz et al. 2017) and because there was of change in prey with growth throughout these developmental stages

(Table 3). The increased feeding intensity at lower surface water temperatures (ESM Fig. S1b) might be explained by the fact that the digestive rate of larvae is reduced under conditions of low water temperature, allowing more food to linger in the digestive tracts. Path analysis was used in this work to prevent misleading univariate analyses, and the effects of water temperature and larval body length on feeding intensities and the strength of other components were assessed separately.

Many marine fish larvae spawning around the Tsugaru Strait feed on copepod nauplii at the initial feeding stage, and often low feeding intensities are observed (e.g., Miyamoto et al. 1993; Takatsu et al. 1995; 2002; 2007; Hasegawa et al. 2003; Hiraoka et al. 2005; Hashimoto et al. 2011; Nanjo et al. 2017; Gao et al. 2020). In contrast, larvae of the Japanese sandfish *Arctoscopus japonicus* hatch at a large NL (approx. 12 mm) and feed primarily on

calanoid copepodites, with no starving larvae during the first feeding stage (Komoto et al. 2011). *Pleurogrammus azonus* was particularly unusual in that only 24% of large yolk-sac stage larvae had empty digestive tracts at the start of feeding in this study. *Pleurogrammus azonus* fed on *Oithona* spp. copepodites, particularly *O. similis* copepodites. *Oithona similis* is cosmopolitan species that lives in subarctic seas and preferentially consumes ciliates over other components of the nano- and microplankton, and the diet is coupled to microbial loop rather than grazing food chain (Turner 2004; Castellani et al. 2005; Balazy et al. 2021). The timing of the spring phytoplankton bloom and the abundance of copepods vary substantially from year to year (see, for example, Yamaoka et al. 2019; Umezawa et al. 2023), and *O. similis* has a lower rate of density growth throughout the bloom period than does calanoid copepods (Yamaoka et al. 2019). One reason *P. azonus* hatches in January and February in the coastal areas of the Matsumae Peninsula may be that the large yolk-sac (the initial feeding stage) larvae use large-sized *O. similis* copepodites on the microbial loop rather than small-sized copepod nauplii to avoid being forced to shift prey immediately after the initial feeding period. After February, *P. azonus* preflexion- and flexion-stage larvae would be able to adapt flexibly to yearly oscillations in the timing of contact with the bloom period by exploiting the calanoid copepods, which are numerous in the grazing food chain. In other words, *P. azonus* most likely has a reproductive strategy that involves using as many copepods as possible, which grow in size and density during the spring bloom. Because *O. similis* has a smaller body size than calanoid copepods, the former would be easy prey for small larvae and poorly swimming larvae during the initial feeding stage, whereas the latter would be a more efficient food source for the well-developed larvae.

This study clarifies, for the first time, the spatiotemporal distribution and feeding ecology of *P. azonus* larvae from the earliest feeding stage, as well as the mechanisms that produce changes in feeding intensity. In the future, we will used otolith increment analysis to clarify the yearly variation in the growth rate of field-collected *P. azonus* larvae (Marannu et al. 2017), find the relationship between the timing of reduced larval feeding intensity and growth rate, and discover when fluctuations in recruitment occur.

## Declarations

## References

Anderson JT (1988) A review of size dependent survival during pre-recruit stages of fishes in relation to recruitment. J Northw Atl Fish Sci 8:55–66

Balazy K, Boehnke R, Trudnowska E, Søreide JE, Błachowiak-Samołyk K (2021) Phenology of *Oithona similis* demonstrates that ecological flexibility may be a winning trait in the warming Arctic. Sci Rep 11:18599

Campana SE (1996) Year-class strength and growth rate in young Atlantic cod *Gadus morhua*. Mar Ecol Prog Ser 135:21–26

Castellani C, Irigoien X, Hariis RP, Lampitt RS (2005) Feeding and egg production of *Oithona similis* in the North Atlantic. Mar Ecol Prog Ser 288:173–182

Chambers RC, Waiwood KG (1996) Maternal and seasonal differences in egg sizes and spawning characteristics of captive Atlantic cod, *Gadus morhua*. Can J Fish Aquat Sci 53:1986–2003

Champalbert G, Koutsikopoulos C (1995) Behavior, transport and recruitment of Bay of Biscay sole (*Solea solea*): laboratory and field studies. J Mar Biol Assoc UK 75:93–108

Cornwell LE, Fileman ES, Bruun JT, Hirst AJ, Tarran GA, Findlay HS, Lewis C, Smyth TJ, McEvoy AJ, Atkinson A (2020) Resilience of the copepod *Oithona similis* to climatic variability: egg production, mortality, and vertical habitat partitioning. Front Mar Sci 7:29. https://doi.org/10.3389/fmars.2020.00029

Cushing DH, Dickson RR (1976) The biological response in the sea to climatic change. Adv Mar Biol 14:1–112

Davydova SV, Shebanova MA, Andreeva EN (2007) Summer-Autumn ichthyoplankton of the Sea of Okhotsk and the Sea of Japan and special traits of feeding of fish larvae and fry in 2003–2004. J Ichthyol 47:520–532

Faillettaz R, Durand E, Paris CB, Koubbi P, Irisson J-O (2017) Swimming speeds of Mediterranean settlement-stage fish larvae nuance Hjort's aberrant drift hypothesis. Limnol Oceanogr 63:509-523. https://doi.org/10.1002/lno.10643

Fukuhara O, Fushimi T (1983) Development and early life history of the greenlings *Hexagrammos otakii* (Pices: Hexagrammidae) reared in the laboratory. Nippon Suisan Gakkaishi 49:1843–1848

Gao W, Nakaya M, Takatsu T, Takeya Y, Noro K (2020) Feeding habits of larval yellow goosefish *Lophius litulon* around Shimokita Peninsula and in Funka Bay. Aquacult Sci. 68:275-277. https://doi.org/10.11233/aquaculturesci.68.275

Haldorson L, Prichett M, Paul AJ, Ziemann D (1993) Vertical distribution and migration of fish larvae in a Northeast Pacific bay. Mar Ecol Prog Ser 101:67–80

Hasegawa A, Takatsu T, Imura K, Nanjo N, Takahashi T (2003) Feeding habits of Japanese flounder *Paralichthys olivaceus* larvae in

Mutsu Bay, northern Japan. Nippon Suisan Gakkaishi 69:940–947 (in Japanese with English abstract)

Hashimoto Y, Maeda A, Oono Y, Kano Y, Takatsu T (2011) Feeding habits of two-flatfish-species larvae in Funka Bay, Japan—importance of *Oikopleura* as prey. Bull Plankton Soc Japan 58:165–177 (in Japanese with English abstract)

Higashitani T, Takatsu T, Nakaya M, Joh M, Takahashi T (2007) Maternal effects and larval survival of marbled sole *Pseudopleuronectes yokohamae*. J Sea Res 58:78–89

Hirano Y (1947) About Arabesque greenling *Pleurogrammus azonus* in Hokkaido. Hokusuishi Geppo 4:10–21 (in Japanese)

Hiraoka Y, Takatsu T, Kurifuji A, Imura K, Takahashi T (2005) Feeding habits of pointhead flounder *Cleisthenes pinetorum* larvae in and near Funka Bay, Hokkaido, Japan. Bull Jpn Soc Fish Oceanogr 69:156–164

Hjort J (1914) Fluctuations in the great fisheries of northern Europe, viewed in the light of biological research. Rapports et procès-verbaux des réunions, Conseil International pour l'Exploration de la Mer, vol 20. Høst and Andr. Fred. Høst & Søn, Copenhagen

Hoshino N, Takashima T, Watanobe M, Fujioka T (2009) Age-structures and catch fluctuations of Arabesque greenling (*Pleurogrammus azonus*) in the coastal area of southern Hokkaido, Japan. Sci Rep Hokkaido Fish Exp Stn 76:1–11 (in Japanese with English abstract)

Houde ED (1987) Fish early life dynamics and recruitment variability. Am Fish Soc Symp 2:17–29

Hunter JR (1981) Feeding ecology and predation of marine fish larvae. In: Lasker R (ed) Marine fish larvae. Washington Sea Grant Program, Washington DC, pp 33–77

Incze LS, Aas P, Ainaire T (1996) Distributions of copepod nauplii and turbulence on the southern flank of Georges Bank: implications for feeding by larval cod (*Gadus morhua*). Deep Sea Res II 43:1855–1873

Irie T (1983) Spawning grounds for greenling *Pleurogrammus azonus* in Hidaka, off the Pacific coast of Hokkaido. Bull Hokkaido Reg Fish Res Lab 48:1–9 (in Japanese with English abstract)

Joh M, Joh T, Matsu-ura T, Takatsu T (2008) Validation of otolith increment formation and the growth rate of fat greenling larvae. Aquacult Sci 56:157–166. https://doi.org/10.11233/aquaculturesci.56.157

Joh M, Takatsu T, Nakaya M, Yoshida N, Nakagami M (2009) Comparison of the nutritional transition date distributions of marbled sole larvae and juveniles in Hakodate Bay. Hokkaido Fish Sci 75:619–628

Joh M, Nakaya M, Yoshida N, Takatsu T (2013) Interannual growth differences and growth-selective survival in larvae and juveniles of marbled sole *Pseudopleuronectes yokohamae*. Mar Ecol Prog Ser 494:267–279

Kajiwara K, Nakaya M, Suzuki K, Kano Y, Takatsu T (2022) Effect of egg size on the growth rate and survival of wild walleye pollock *Gadus chalcogrammus* larvae. Fish Oceanogr 31:238–254

Kambara H (1957) Studies on Arabesque greenling *Pleurogrammus azonus* Jordan et Metz (II)—spawning ecology. Hokusuishi Geppo 14:359–379

Kano Y, Takatsu T, Hashimoto Y, Inagaki Y, Nakatani T (2015) Annual variation in otolith increment widths of walleye pollock (*Gadus chalcogrammus*) larvae in Funka Bay, Hokkaido, Japan. Fish Oceanogr 24:325–334

Kjesbu OS, Solemdal P, Bratland P, Fonn M (1996) Variation in annual egg production in individual captive Atlantic cod (*Gadus morhua*). Can J Fish Aquat Sci 53:610–620

Komoto R, Kudou K, Takatsu T (2011) Vertical distribution and feeding habits of Japanese sandfish (*Arctoscopus japonicus*) larvae and juveniles off Akita Prefecture in the Sea of Japan. Aquacult Sci 59:615–630. https://doi.org/10.11233/aquaculturesci.59.615 (in Japanese with English abstract)

Kyushin K (1977) About early life history of Arabesque greenling, *Pleurogrammus azonus* Jordan et Metz. Bull Jpn Soc Fish Oceanogr 31:29–32 (in Japanese)

Litvak MK, Leggett WC (1992) Age and size-selective predation on larval fishes: the bigger-is-better hypothesis revisited. Mar Ecol Prog Ser 81:13–24

Marannu S, Nakaya M, Takatsu T, Takabatake S, Joh M, Suzuki Y (2017) Otolith microstructure of Arabesque greenling *Pleurogrammus azonus*: a species with a long embryonic period. Fish Res 194:129–134

Miller TJ, Crowder LB, Rice JA, Marschall EA (1988) Larval size and recruitment mechanisms in fishes: toward a conceptual framework. Can J Fish Aquat Sci 45:1657–1670

Miyamoto T, Takatsu T, Nakatani T, Maeda T, Takahashi T (1993) Distribution and food habits of eggs and larvae of *Hippoglossoides dubius* in Funka Bay and its offshore waters, Hokkaido. Bull Jpn Soc Fish Oceanogr 57:1–14 (in Japanese with English abstract)

Nagasawa T, Saito M (2014) Hexagrammidae. In: Okiyama M (ed) An atlas of early stage fishes in Japan, 2nd edn. Tokai University Press, Hadano, pp 1009–1018 (in Japanese)

Nakaya M, Marannu S, Inagaki Y, Kajiwara K, Sato Y, Suzuki K, Takatsu T (2017) Relationship between temperature and embryonic period of Arabesque greenling *Pleurogrammus azonus*. Aquacult Sci 65:247–250. https://doi.org/10.11233/aquaculturesci.65.247

Nanjo N, Takatsu T, Imura K, Itoh K, Takeya Y, Takahashi T (2017) Feeding, somatic condition and survival of sand lance *Ammodytes* sp. larvae in Mutsu Bay. Japan Fish Sci 83:199–214

Natsume M (1995) Migration of Arabesque greenling *Pleurogrammus azonus* from Okushiri Island in Hokkaido. Sci Rep Hokkaido Fish Exp Stn 47:7–13 (in Japanese with English abstract)

Natsume M (2003) Arabesque greenling *Pleurogrammus azonus* Jordan and Metz. In: Ueda Y et al (eds) Fisheries and aquatic life in Hokkaido. The Hokkaido Shimbun Press, Sapporo, pp 196–201 (in Japanese)

Nishiyama T, Hirano K (1983) Estimation of zooplankton weight in the gut of larval walleye pollock (*Theragra chalcogramma*). Bull Plankton Soc Japan 30:159–170

Odamaki M (1985) Tides and currents. In: Editorial committee of the "Coastal Ocean Journal" of the Coastal Ocean Research Division of the Japan Society of Oceanography (ed) Japan national coastal oceanography. Tokai University Press, Tokyo, pp 145–149 (in Japanese)

Okiyama M (1965) A preliminary study on the fish eggs and larvae occurring in the Sado Strait, Japan Sea, with some remarks on the vertical distribution of some Fishes. Bull Jap Sea Reg Fish Res Lab 15:13–37 (in Japanese with English abstract)

Olla BL, Davis MW (1990) Effects of physical factors on the vertical distribution of larval walleye pollock (*Theragra chalcogramma*) under controlled laboratory conditions. Mar Ecol Prog Ser 63:105–112

Pearre Jr S (1980) The copepod width-weight relation and its utility in food chain research. Can J Zool 58:1884–1891

Pepin P, Shears TH, de Lafontaine Y (1992) Significance of body size to the interaction between a larval size (*Mallotus villosus*) and a vertebrate predator (*Gasterosteus aculeatus*). Mar Ecol Prog Ser 81:1–12

Pinkas L, Oliphant MS, Inverson ILK (1971) Food habits of albacore, bluefin tuna, and bonito in Californian waters. Fish Bull 152:1–105

Ponton D, Fortier L (1992) Vertical distribution and foraging of marine fish larvae under the ice cover of southeastern Hudson Bay. Mar Ecol Prog Ser 81:215–227

Porter SM, Ciannelli L, Hillgruber N, Bailey KM, Chan K-S, Canino MF, Haldorson LJ (2005) Environmental factors influencing larval walleye pollock *Theragra chalcogramma* feeding in Alaska waters. Mar Ecol Prog Ser 302:207–217

Sano M (1984) Reproduction of walleye pollock and Arabesque greenling in and around the Soya Strait. Bull Coastal Oceanogr 22:40–49. https://doi.org/10.32142/engankaiyo.22.1_40 (in Japanese)

Solemdal P (1997) Maternal effect—a link between the past and the future. J Sea Res 37:213–227

Takashima T, Hoshino N, Itaya K, Maeda K, Miyashita K (2013) Age validation using sectioned otoliths and age-size relationship for the Northern Hokkaido stock of the Arabesque greenling *Pleurogrammus azonus*. Nippon Suisan Gakkaishi 79:383–393 (in Japanese with English abstract)

Takashima T, Okada N, Asami H, Hoshino N, Shida O, Miyashita K (2016) Maturation process and reproductive biology of female Arabesque greenlings *Pleurogrammus azonus* in the Sea of Japan, off the west coast of Hokkaido. Fish Sci 82:225–240

Takasuka A, Aoki I, Mitani I (2003) Evidence of growth-selective predation on larval Japanese anchovy *Engraulis japonicus* in Sagami Bay. Mar Ecol Prog Ser 252:223–238

Takatsu T (1998) Early life history of *Gadus macrocephalus* in Mutsu Bay. PhD dissertation, Hokkaido University, Hakodate. https://doi.org/10.11501/3146391 (in Japanese)

Takatsu T, Nakatani T, Mutoh T, Takahashi T (1995) Feeding habits of Pacific cod larvae and juveniles in Mutsu Bay, Japan. Fish Sci 61:415–422

Takatsu T, Nakatani T, Miyamoto T, Kooka K, Takahashi T (2002) Spatial distribution and feeding habits of Pacific cod (*Gadus macrocephalus*) larvae in Mutsu Bay, Japan. Fish Oceanogr 11:90–101

Takatsu T, Suzuki Y, Shimizu A, Imura K, Hiraoka Y, Shiga N (2007) Feeding habits of larval stone flounder *Platichthys bicoloratus* in Mutsu Bay, Japan. Fish Sci 73:142–155

Toba Y, Tomizawa K, Kurasawa Y, Hanawa K (1982) Seasonal and year-to-year variability of the Tsushima-Tsugaru Warm Current System with its possible cause. La Mer 20:41–51

Tsujisaki H, Kambara H (1958) Studies on Arabesque greenling *Pleurogrammus azonus* Jordan et Metz (VII)—migration. Hokusuishi Geppo 15:3–18 (in Japanese)

Turner JT (2004) The importance of small planktonic copepods and their roles in pelagic marine food webs. Zool Stud 43:255–266

Umezawa S, Tozawa M, Nosaka Y, Nomura D, Onishi H, Abe H, Takatsu T, Ooki A (2023) Significant nutrient consumption in the dark subsurface layer during a diatom bloom: a case study on Funka Bay, Hokkaido, Japan. Biogeosciences 20:421–438

van der Veer HW, Bergman MJN (1987) Predation by crustaceans on a newly settled 0-group plaice *Pleuronectes platessa* population in the western Wadden Sea. Mar Ecol Prog Ser 35:201–215

Watanabe Y, Zenitani H, Kimura R (1995) Population decline of the Japanese sardine *Sardinops melanostictus* owing to recruitment failures. Can J Fish Aquat Sci 52:1609–1616

Yamaoka K, Takatsu T, Suzuki K, Kobayashi N, Ooki A, Nakaya M (2019) Annual and seasonal changes in the assemblage of planktonic copepods and appendicularians in Funka Bay before and after intrusion of Coastal Oyashio Water. Fish Sci 85:1077–1087